IOPscience iopscience.iop.org

Home Search Collections Journals About Contact us My IOPscience

Enhanced Stimulated Emission from Optically Pumped Gallium Nitride Nanopillars

This content has been downloaded from IOPscience. Please scroll down to see the full text.

2011 Appl. Phys. Express 4 022102

(http://iopscience.iop.org/1882-0786/4/2/022102)

View the table of contents for this issue, or go to the journal homepage for more

Download details:

IP Address: 140.113.38.11

This content was downloaded on 25/04/2014 at 00:51

Please note that terms and conditions apply.

Applied Physics Express **4** (2011) 022102
DOI: 10.1143/APEX.4.022102

Enhanced Stimulated Emission from Optically Pumped Gallium Nitride Nanopillars

Ming-Hua Lo[1,2], Yuh-Jen Cheng[1,2*], Hao-Chung Kuo[1], and Shing-Chung Wang[1]

[1] *Department of Photonics and Institute of Electro-Optical Engineering, National Chiao Tung University, Hsinchu, Taiwan 300, R.O.C.*
[2] *Research Center for Applied Sciences, Academia Sinica, Taipei, Taiwan 115, R.O.C.*

Received December 2, 2010; accepted January 12, 2011; published online February 1, 2011

We report the observation of an enhanced stimulated emission from optically pumped GaN nanopillars. The nanopillars were fabricated from an epitaxial wafer by patterned etching followed by crystalline regrowth. When the sample was optically excited, a strong stimulated emission peak emerged from a broad spontaneous emission background. The emission was attributed to electron–hole plasma gain at high carrier density. The emission slope efficiency was greatly enhanced by 20 times compared with a GaN substrate under the same pumping configuration. We remark that the enhancement is due to better gain and photon interaction from the multiple scattering of photons among nanopillars.
© 2011 The Japan Society of Applied Physics

Gallium nitride has attracted great research interests owing to its effective emission properties and promising applications in UV to blue optoelectronic devices. In the past, GaN devices were typically built from epitaxial thin film in a two-dimensional structure. Recently, devices in one-dimensional nanostructure have gained substantial attention for their novel properties and potential applications.[1–3] The nanodevices, known as nanowires or nanopillars, can be fabricated by self-assembled or selective-area growth by molecular beam epitaxy and metalorganic chemical vapor deposition (MOCVD).[4–6] The as-grown nanowires or nanopillars have shown improved material quality, size confinement effect, and significantly enhanced light emission properties.[4,7–9] Stimulated emission has been reported from optically pumped GaN nanowires.[4,10,11)]

In this letter, we report a different technique to fabricate GaN nanopillars and the observation of enhanced stimulated emission by optical pumping. The nanopillars were fabricated from an epitaxial wafer by self-assembled Ni masked pattern etching, followed by a MOCVD regrowth to form crystalline hexagonal nanopillars. The regrowth process was important for improving the material quality of the originally etched nanopillars. The nanopillars have an average diameter of 250 nm and a height of 660 nm standing on a GaN substrate. When the sample was optically pumped from the nanopillar end surface by a 355 nm laser with a 37 µm spot size, a strong stimulated emission peak emerged from a broad spontaneous emission background. The emission peak was redshifted from the spontaneous emission peak by about 5 nm. The gain mechanism is attributed to the formation of electron–hole plasma under high-carrier-density excitation. The slope efficiency of stimulated emission was greatly enhanced by 20 times compared with that from a GaN thin film substrate under the same pumping configuration. We remark that the enhancement is due to better gain and photon interaction enabled by the multiple scattering of photons among nanopillars.

The GaN nanopillar sample was fabricated by self-assembled Ni nanomasked etching and crystalline regrowth from a GaN epitaxial substrate. A 300 nm Si_3N_4 thin film was first deposited on a 3 µm GaN thin film substrate by plasma-enhanced CVD, followed by subsequent deposition of a Ni thin film by electron-beam evaporation. The sample was subjected to rapid thermal annealing (RTA) at 850 °C under nitrogen ambiance for 1 min to form self-assembled Ni nanomasks on the Si_3N_4 film surface. Reactive ion etching was conducted to etch the Si_3N_4 film using a CF_4/O_2 gas mixture to transfer the Ni nanomask pattern down to the Si_3N_4 layer. The sample was subsequently etched down to GaN by an inductively coupled plasma reactive ion etching system (SAMCO ICP-RIE 101iPH) operated at 13.5 MHz under a gas mixture of $Cl_2/Ar = 50/20$ sccm for 2 min to form nanopillars. The ICP source power and the bias power of the ICP-RIE system were set at 400 and 100 W, respectively. The sample was dipped into a nitric acid solution (HNO_3) at 100 °C for 5 min to remove Ni nanomasks. The etched nanopillars have an average height 580 nm and diameter 150 nm. The density of GaN nanopillars is estimated to be about $8.5 \times 10^8/cm^2$. Finally, the etched GaN nanopillars were put back by MOCVD epitaxial regrowth. The Si_3N_4 mask was intentionally left on top of nanopillars to prevent the growth in the vertical direction. Figures 1(a) and 1(b) are the scanning electron microscope (SEM) images of the fabricated nanopillars. The irregular shape was originated from the self-assembled Ni nanomasks. The regrowth grew additional GaN on the side walls of the etched pillars and formed hexagonal *M*-plane $\{11\bar{2}0\}$ crystalline facets, as shown in the top view of Fig. 1(a). It also formed inclined *R*-plane facets $\{11\bar{2}2\}$ close to the top of the nanopillars. The purpose of regrowth was to reduce surface defects created during the ICP-RIA etching process. After regrowth, the height and average diameter of the nanopillars were 660 and 250 nm, respectively.

The nanopillar sample was optically excited by a tripled Nd:YAG 355 nm pulse laser at room temperature. The pulse width was 0.5 ns and the pulse repetition rate was 1 kHz. The laser beam was focused by a 15× UV microscope objective on to the sample surface. The nanopillars were pumped from their end surfaces and the pump spot at sample surface had a Gaussian intensity profile with a $1/e^2$ diameter of 37 µm. Given the distribution of nanopillars, there were thousands of pillars covered by the pump spot. The photoluminescent (PL) spectrum was collected by the same UV objective and coupled into an optical fiber connected to the input of a spectrometer (Jobin Yvon IHR320).

The PL spectra at various pump power intensities are shown in Figs. 2(a)–2(c), where the legends are pump intensity levels in unit MW/cm^2. At low pump intensity [0.8 MW/cm^2 curve in Fig. 2(a)], the spontaneous emission spectrum has a maximum at around 364 nm, which is the nominal exciton transition wavelength of GaN.[12,13] As pump intensity increases, an emission start to emerge at

*E-mail address: yjcheng@sinica.edu.tw

© 2011 The Japan Society of Applied Physics

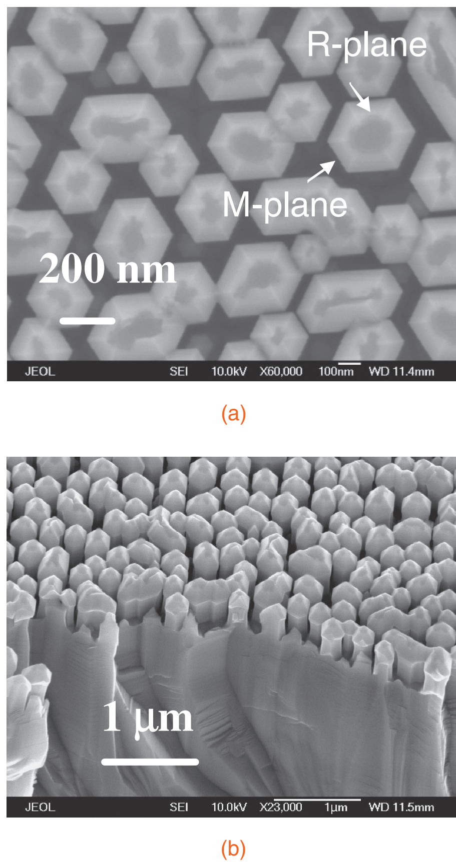

Fig. 1. (a) SEM top view image of nanopillars. (b) SEM angle view image of nanopillars.

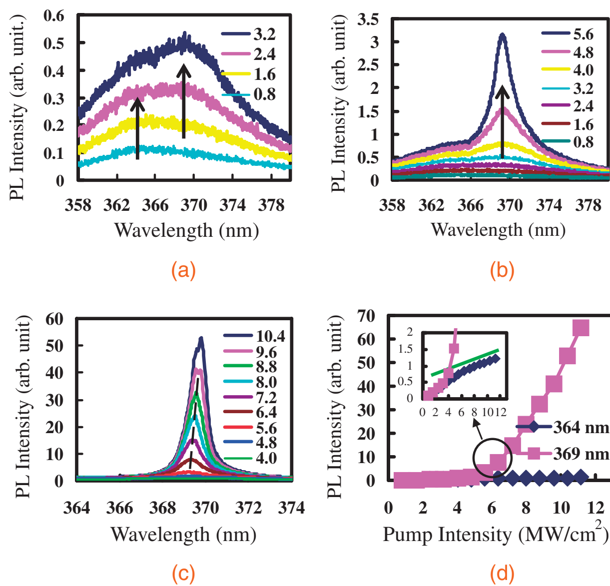

Fig. 2. (a)–(c) PL spectra of optically pumped nanopillars at increasing pump intensity. The legends are pump intensity levels in MW/cm^2. (d) 364 and 369 nm emission peak intensity vs pump intensity. Inset is the zoom in at vertical scale to make the thin film emission level visible. The straight line is a visual guide to show the change in slope efficiency.

around 369 nm. As pump intensity increases further [Fig. 2(b)], the intensity at 369 nm increases with a fast growing rate and has a large jump for the pump intensity step from 4.8 to 5.6 MW/cm^2, which indicates a threshold of stimulated emission. The 364 nm intensity, regarded as the spontaneous emission background, in contrast, only increases in steady increments. Above the threshold, the 369 nm emission continues to increase in large steps and at the same time redshifts slightly, as shown in Fig. 2(c) where the dotted vertical line is a visual guide to show the slight redshift. The emission intensity at 364 nm becomes negligible compared with that at 369 nm. Figure 2(d) shows the 364 and 369 nm PL peak intensities versus pump intensity, where Lorentzian curve fitting is used to obtain the emission peak values. Compared to the steady increase of 364 nm intensity, the 369 nm emission peak clearly shows an onset of stimulated emission. The stimulated emission linewidth is about one nm. The inset in Fig. 2(d) shows the slight slow down of the slope efficiency of 364 nm spontaneous emission above the threshold. This is because the onset of the stimulated emission provides an additional decay channel for the excited carriers and leads to a slower increase of carrier density. As a result, the 364 nm spontaneous emission increases at a slower rate above the threshold. The pump intensity for the onset of stimulated emission is about 5.5 MW/cm^2. Given the absorption coefficient of $1 \times 10^5\ cm^{-1}$ and carrier recombination coefficient of $1.3 \times 10^{-8}\ cm^3\ s^{-1}$ from reported studies,[14,15] the excited carrier density at the threshold pump intensity is about $8.6 \times 10^{18}\ cm^{-3}$. This is higher than the typical reported Mott transition density of $1.8 \times 10^{18}\ cm^{-3}$.[16] At such a high carrier density, electron–hole plasma is the major gain mechanism and the band gap will decrease with increasing carrier density due to the carrier screening effect.[17,18] This explains the observed slight redshift of peak emission with increasing pump intensity.[16] We therefore remark that electron–hole plasma is the main gain mechanism for the observed stimulated emission in our nanopillar sample.

For comparison, a GaN substrate and an etched nanopillar sample without crystalline regrowth were also pumped by the same optical setup. The emission properties of the etched nanopillar sample without regrowth are very similar to those described previously for the regrown nanopillar sample except that its slope efficiency is significantly lower. This is because the surface defect density is higher without regrowth. The emission properties from a bulk GaN substrate are, however, significantly different. The PL spectrum versus pump intensity is shown in Fig. 3(a). At a low pump intensity, the PL spectrum shows a maximum around the exciton transition wavelength. The wavelength is slightly shorter than that in the nanopillar sample. The slight variation could be due to the strain difference left from epitaxial growth between these two samples. As the pump intensity increases, a peak emerges at 369 nm wavelength similar to the nanopillar case but with a much slower increasing rate. The emergence of the 369 nm peak is also around a pump intensity of 5.5 MW/cm^2, similar to what is observed for the nanopillar sample. It is worth noting the drastic spectral difference between Figs. 3(a) and 2(c). The emerging 369 nm peak remains comparable to the exciton peak in thin film GaN, whereas it is large enough to make exciton emission peak negligible in the nanopillar sample. The stimulated emission efficiency is greatly enhanced in the

© 2011 The Japan Society of Applied Physics

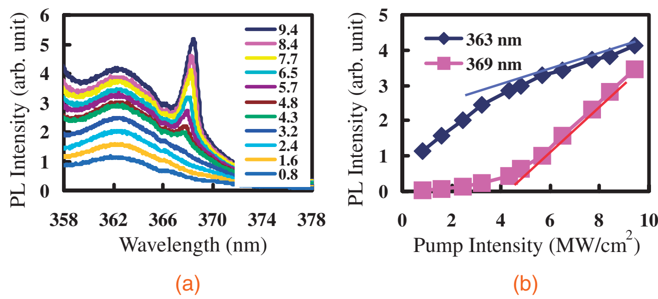

Fig. 3. (a) PL spectra of optically pumped GaN thin film substrate at increasing pump intensity. (b) 363 and 369 nm emission peak intensity vs pump intensity. The straight lines are visual guides to show the changes in slope efficiencies.

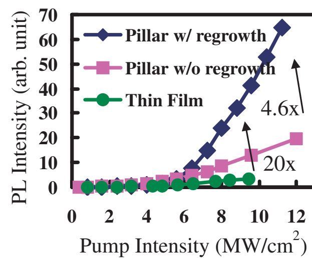

Fig. 4. PL peak intensity of 369 nm emission versus pump intensity for nanopillar with regrowth, without regrowth, and GaN thin film sample. The slope efficiency of nanopillars with regrowth is enhanced by 4.6 and 20 times compared to without regrowth and thin film sample, respectively.

nanopillar sample. The exciton emission and the emerging 369 nm peak intensity versus pump power are shown in Fig. 3(b). The slope efficiency of the exciton emission slightly slows down after the emergence of the 369 nm peak, which is due to the same mechanism as mentioned previously. The onset of the 369 nm stimulated emission is not as strong as that in the nanopillar sample. The 369 nm peak intensities versus pump intensity for the nanopillar with regrowth, without regrowth, and thin film samples are shown in Fig. 4. The stimulated emission slope efficiency for the nanopillar sample with regrowth is significantly enhanced by 4.6 times compared with nanopillar without regrowth, and by 20 times compared with thin film sample. The regrowth significantly reduces surface defects and leads to better emission efficiency. We remark that the large 20× enhancement compared to thin film sample is due to better carrier confinement provided by the nanopillar structure and the increase in photon sojourn time from the multiple scattering among nanopillars. As a result, photons have more chance to interact with gain and the stimulated emission efficiency is greatly enhanced. This is in contrast to the bulk GaN substrate where there is no lateral confinement to enhance gain and photon interaction.

In summary, we have fabricated GaN nanopillars by patterned etching followed by crystalline regrowth from an epitaxial substrate. We observed a large stimulated emission enhancement from the nanopillar sample when it was pumped by a 355 nm pulsed laser. The gain mechanism for the stimulated emission is attributed to electron–hole plasma. The stimulated emission efficiency is greatly enhanced by 20 times compared with that from a GaN thin film substrate under the same pumping condition. We remark that this is due to better gain and photon interaction provided by the nanopillar structure.

Acknowledgments This work was financially supported by the National Science Council of Taiwan under contract No. NSC NSC97-2112-M-001-027-MY3, and the Academia Sinica Nano-program.

1) F. Qian, S. Gradečak, Y. Li, C.-Y. Wen, and C. M. Lieber: Nano Lett. **5** (2005) 2287.
2) R. Chen, H. D. Sun, T. Wang, K. N. Hui, and H. W. Choi: Appl. Phys. Lett. **96** (2010) 241101.
3) H. Sekiguchi, K. Kishino, and A. Kikuchi: Appl. Phys. Lett. **96** (2010) 231104.
4) A. Kikuchi, K. Yamano, M. Tada, and K. Kishino: Phys. Status Solidi B **241** (2004) 2754.
5) S. D. Hersee, X. Sun, and X. Wang: Nano Lett. **6** (2006) 1808.
6) L. W. Tu, C. L. Hsiao, T. W. Chi, I. Lo, and K. Y. Hsieh: Appl. Phys. Lett. **82** (2003) 1601.
7) H. Sekiguchi, T. Nakazato, A. Kikuchi, and K. Kishino: J. Cryst. Growth **300** (2007) 259.
8) Y. Sun, Y.-H. Cho, H.-M. Kim, and T. W. Kang: Appl. Phys. Lett. **87** (2005) 093115.
9) Y. Kawakami, S. Suzuki, A. Kaneta, M. Funato, A. Kikuchi, and K. Kishino: Appl. Phys. Lett. **89** (2006) 163124.
10) J. C. Johnson, H.-J. Choi, K. P. Knutsen, R. D. Schaller, P. D. Yang, and R. J. Saykally: Nat. Mater. **1** (2002) 106.
11) S. Gradečak, F. Qian, Y. Li, H.-G. Park, and C. M. Liebera: Appl. Phys. Lett. **87** (2005) 173111.
12) S. Shokhovets, K. Köhler, O. Ambacher, and G. Gobsch: Phys. Rev. B **79** (2009) 045201.
13) A. J. Fischer, W. Shan, J. J. Song, Y. C. Chang, R. Horning, and B. Goldenberg: Appl. Phys. Lett. **71** (1997) 1981.
14) J. F. Muth, J. H. Lee, I. K. Smagin, R. M. Kolbas, H. C. Casey, B. P. Keller, U. K. Mishra, and S. P. DenBaars: Appl. Phys. Lett. **71** (1997) 2572.
15) F. Binet, J. Y. Duboz, E. Rosencher, F. Scholz, and V. Harle: Appl. Phys. Lett. **69** (1996) 1202.
16) F. Binet, J. Y. Duboz, J. Off, and F. Scholz: Phys. Rev. B **60** (1999) 4715.
17) S. Bidnyk, T. J. Schmidt, B. D. Little, and J. J. Song: Appl. Phys. Lett. **74** (1999) 1.
18) K. Kazlauskas, G. Tamulaitis, A. Žukauskas, T. Suski, P. Perlin, M. Leszczynski, P. Prystawko, and I. Grzegory: Phys. Rev. B **69** (2004) 245316.

 © 2011 The Japan Society of Applied Physics